DYNAMIC POSITIONING CONFERENCE
October 7 - 8, 2008

Thrusters

Design of Reliable Steerable Thrusters by Enhanced Numerical Methods and Full Scale Optimization of Thruster – Hull Interaction Using CFD

Dirk Jürgens, Michael Palm, Andreas Amelang, Torsten Moltrecht

Voith Turbo Marine, Heidenheim, Germany

1. Introduction

An optimized propulsion system is important for many offshore operations. The target of Voith Turbo Marine is the development of reliable and efficient thrusters for the offshore industry. Additionally Voith is offering support for the hull design and the prediction of the hydrodynamics of the whole system. Voith is using Computational Fluid Dynamics (CFD) methods ([1], [12]), a simulator of the motions of marine systems and experimental methods [2].

360°- steerable thrusters are widely used in the offshore industry for efficient dynamic positioning. A target for an economical and ecological application of steerable thrusters is the minimization of efficiency losses. The reasons for these losses are 1) interaction effects between thruster and hull, 2) interaction effects between thruster and thruster, 3) momentum and friction losses of the thruster itself and 4) mechanical losses.

This paper focuses on the interaction of thruster and hull. This interaction has been analyzed experimentally and by numerical methods. The target of the research activities was to achieve a better insight into the physical effects of the relevant flow phenomena. Therefore pressure calculations, force determinations and flow visualizations have been carried out, respectively by numerical methods and in the model tank test.

A simple and fast experimental method was developed to analyze the effect of the propeller shaft tilting and the influence of the geometry of the hull.

The scale effect for 360° steerable thrusters working with a very low advance coefficient, or under bollard pull conditions, is important [11]. So far, the knowledge of the interaction is based mainly on studies carried out in model scale. Therefore the main part of the paper shows results of the interaction between thruster and hull for full scale Reynolds number. The analysis was made by solving the Reynolds-averaged Navier-Stokes equations (RANSE) using the commercial Computational Fluid Dynamics (CFD) Code COMET.

In [3], it was shown that the tilting of the nozzle of an offshore thruster reduced the Coanda effect and the interaction between thruster wake and the hull of the offshore platform. One assumes that the tilting of the propeller shaft is more efficient [4] than tilting only the nozzle; because the interaction of screw propeller and nozzle is then not negatively influenced. Therefore only the tilting of the propeller axis has been analyzed.

For the interaction of two thruster, and between thruster and hull, there are many studies known ([5]-[8]), although only a few of them have been carried out with tilted axes, e.g. [9]. The studies on the effect of the tilt angle were mostly carried out for a small number of angles; therefore there are open questions about the change of the flow filed as a function of the tilt angle.

2. Computational Method

The numerical studies have been performed by using the commercial code COMET from CD Adapco [1]. This code is using the finite-volume (FV) method. The flow field is subdivided into a finite number of control volumes (CVs), which can be of an arbitrary polyhedral shape. Figure 1 shows exemplarily the discretization of the propeller surface.

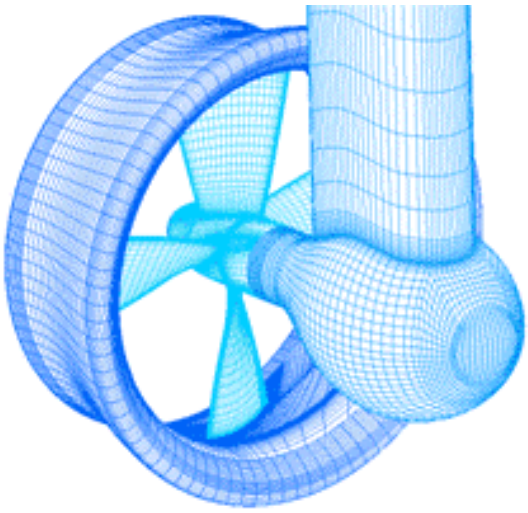

Fig. 1. Discretization mesh of a 360° steerable thruster

The physical model for the flow calculation is based on the Reynolds-averaged Navier-Stokes equations. The effect of the turbulence is calculated by the *k*-ε model.

The hydrodynamic data are calculated by solving the continuity equation, three momentum component equations, and two equations for turbulence properties.
These equations are:

Mass conservation:

$$\frac{\mathrm{d}}{\mathrm{d}t}\int_V \rho \,\mathrm{d}V + \int_S \rho(\mathbf{v}-\mathbf{v}_\mathrm{b})\cdot\mathbf{n}\,\mathrm{d}S = 0$$

Momentum conservation:

$$\frac{\mathrm{d}}{\mathrm{d}t}\int_V \rho\mathbf{v}\,\mathrm{d}V + \int_S \rho\mathbf{v}(\mathbf{v}-\mathbf{v}_\mathrm{b})\cdot\mathbf{n}\,\mathrm{d}S = \int_S (\mathbf{T}-p\mathbf{I})\cdot\mathbf{n}\,\mathrm{d}S + \int_V \rho\mathbf{b}\,\mathrm{d}V$$

Generic transport equation for scalar quantities:

$$\frac{\mathrm{d}}{\mathrm{d}t}\int_V \rho\phi\,\mathrm{d}V + \int_S \rho\phi(\mathbf{v}-\mathbf{v}_\mathrm{b})\cdot\mathbf{n}\,\mathrm{d}S = \int_S \Gamma\nabla\phi\cdot\mathbf{n}\,\mathrm{d}S + \int_V \rho b_\phi\,\mathrm{d}V$$

Where:

- **v** is the fluid velocity vector,
- **n** is the unit vector normal to CV surface,
- *S* is the area and volume *V* of the CV,
- **T** stands for the stress tensor (expressed in terms of velocity gradients and eddy viscosity),
- *p* is the pressure,
- **I** is the unit tensor,
- ϕ stands for the scalar variable (*k* or ε or ω),
- Γ is the diffusivity coefficient,
- **b** is the vector of body forces per unit mass and b_ϕ represents sources or sinks of ϕ.

The above written conservation equations in integral form have to be discretized by numerical approximation. This leads to an algebraic system of equation, solvable on a computer system. Initial and boundary conditions have to be applied to get the relevant flow data: velocity vector, pressure and turbulence data.

Figure 2 shows the pressure distribution of a 360° steerable thruster.

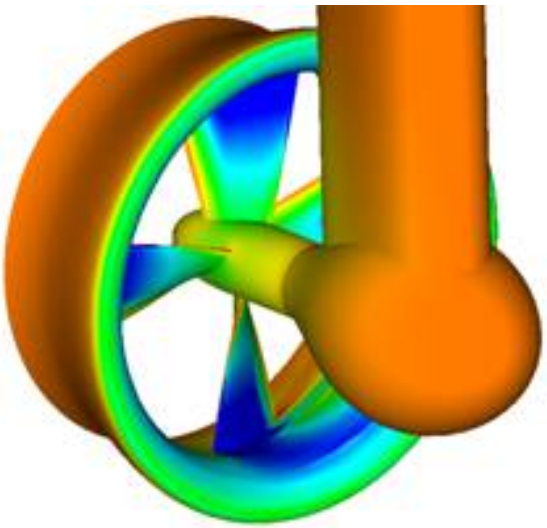

Fig. 2. Calculated pressure distribution of a 360° steerable thruster

The flow is visualized in figure 3 for bollard pull condition. The flow pattern indicates the well known and strong effect of the nozzle.

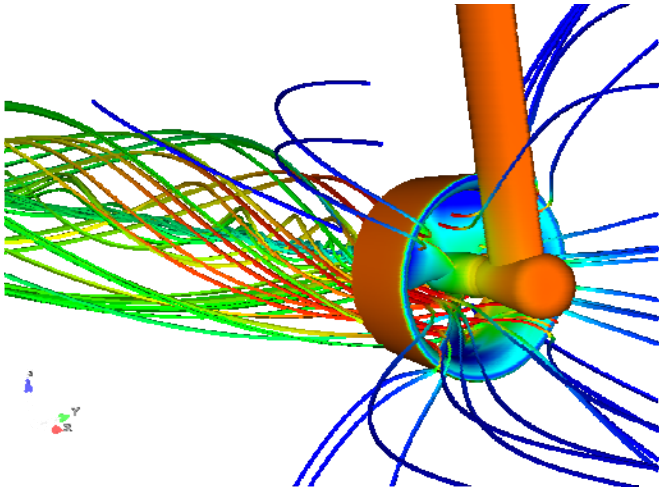

Fig.3 Visualization of the flow pattern of a 360° steerable thruster

The emphasis of the present study is on determining interaction effect thruster and hull. The above explained CFD-method is used to optimize the tilt angle of the propeller axis and to gain more insight into the physics of the interaction between thruster and hull.

3. Numerical study of the interaction between thruster and hull

The calculations have been carried out in full scale for the following propeller parameter:
Diameter of the screw propeller: 4.2 m; RPM: 138

The calculations have been done for the following tilt angles of the propeller axis: 0°, 2°, 4°, 6°, 7°, 8°and 9°.
The calculations were made for a semisubmersible rig consisting of two pontoons with infinite length. The analyzed thruster is mounted at pontoon 1.

The arrangement of the thruster and the two pontoons is shown in figure 4 and 14. Only forces of an azimuth angle of 90°, relative to the pontoon longitudinal axis, have been calculated.

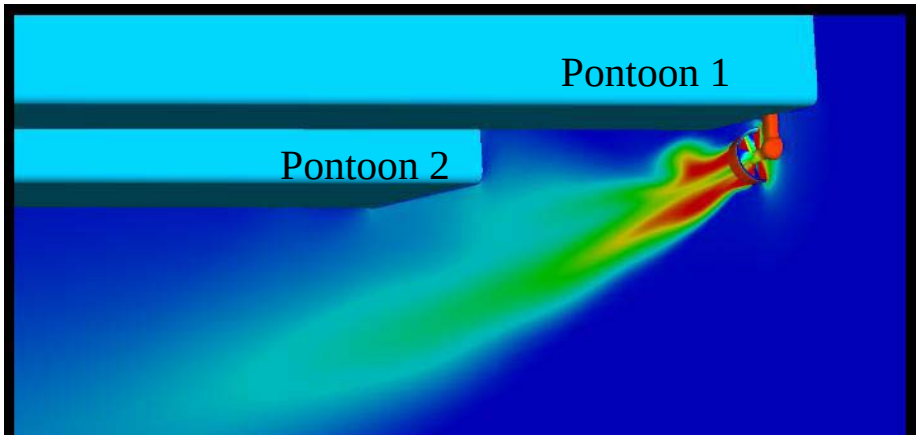

Fig. 4. Arrangement of the pontoons and the thruster with 8° propeller shaft tilting

Figure 5. shows the effect of the tilting angle of the propeller axis on the velocity distribution.

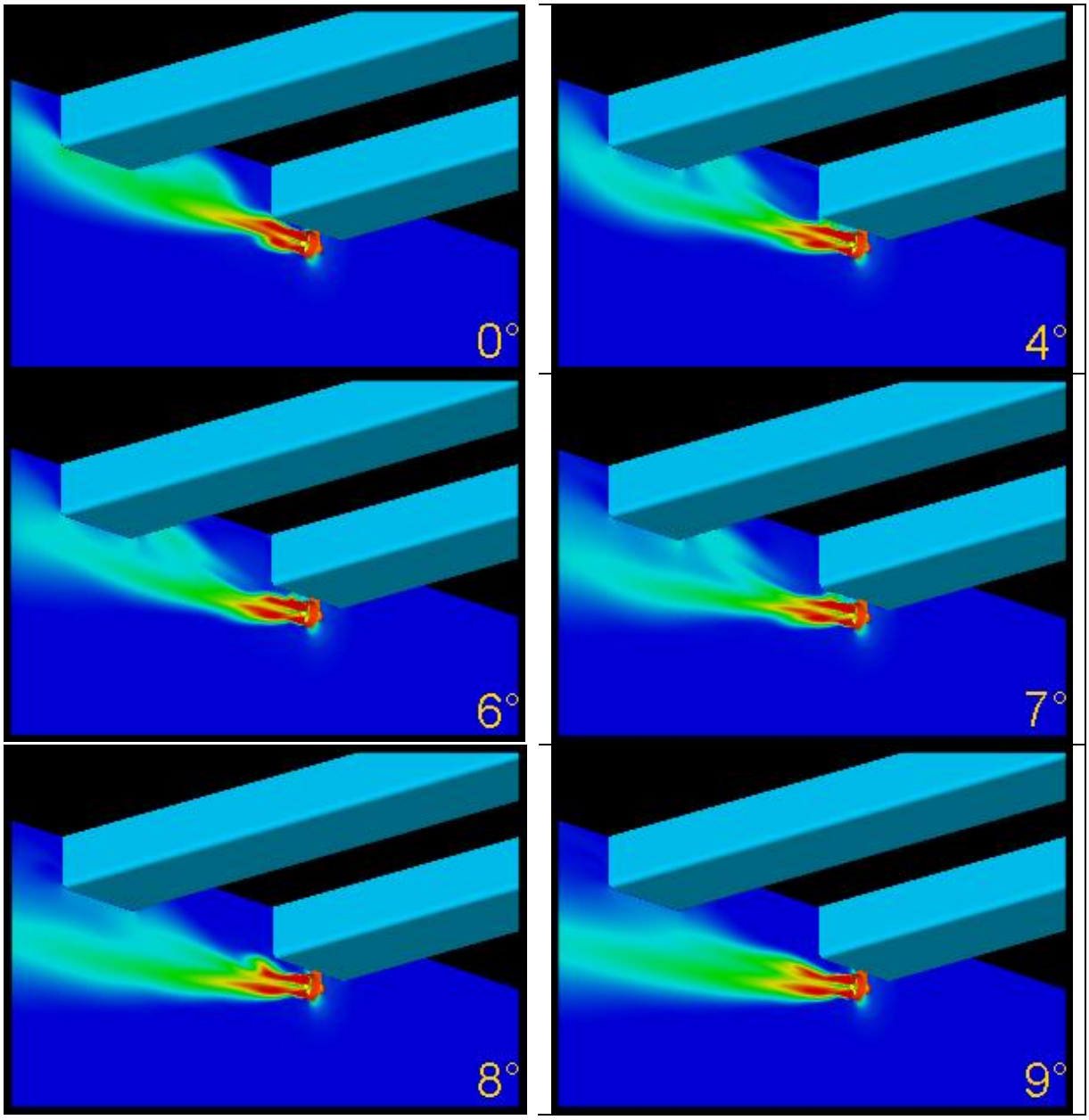

Fig. 5: Velocity distribution as a function of the tilt angle of the propeller axis

There is a strong influence of the tilt angle of the propeller shaft visible on the flow pattern. At 8° there is a change of the flow characteristic and much less interaction between the thruster wake and pontoon 2.

The important question is, how this effect will be reflect in the decisive hydrodynamic forces. Figure 6 shows the total thrust ratio τ as a function of the tilt angle:

$$\tau = \frac{Fh}{Th}$$

Here *Fh* is the resulting total horizontal force, created by the thruster on the platform. This force consists of the thruster force and the thrust deduction due to the interaction effect between thruster and hull. *Th* is the horizontal thrust component of the thruster only. There would be no efficiency loss of the thruster due to the thruster hull interaction if τ were 100%. From 0° to 7° there is a linear increase of the total thrust ratio τ from 54% to 84%. At 8° there is a jump from 84% to 95%. This jump corresponds to the change of the flow pattern as shown in figure 5. Obviously there is a change of the flow characteristic. A closer look will be given by the figures 7 and 8.
There is only very little improvement of 1% in the total thrust ratio τ from 8° to 9° of tilt angle.

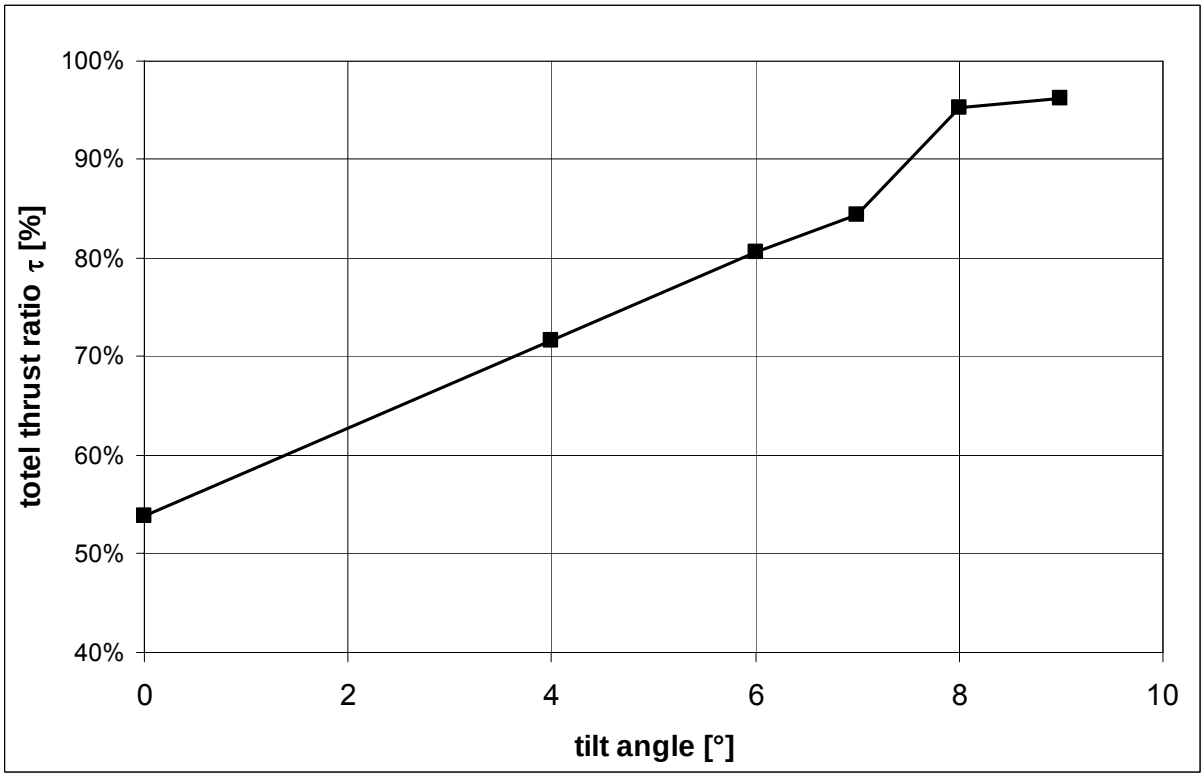

Fig. 6. Total thrust ratio τ as the function of the tilt angle of the propeller shaft

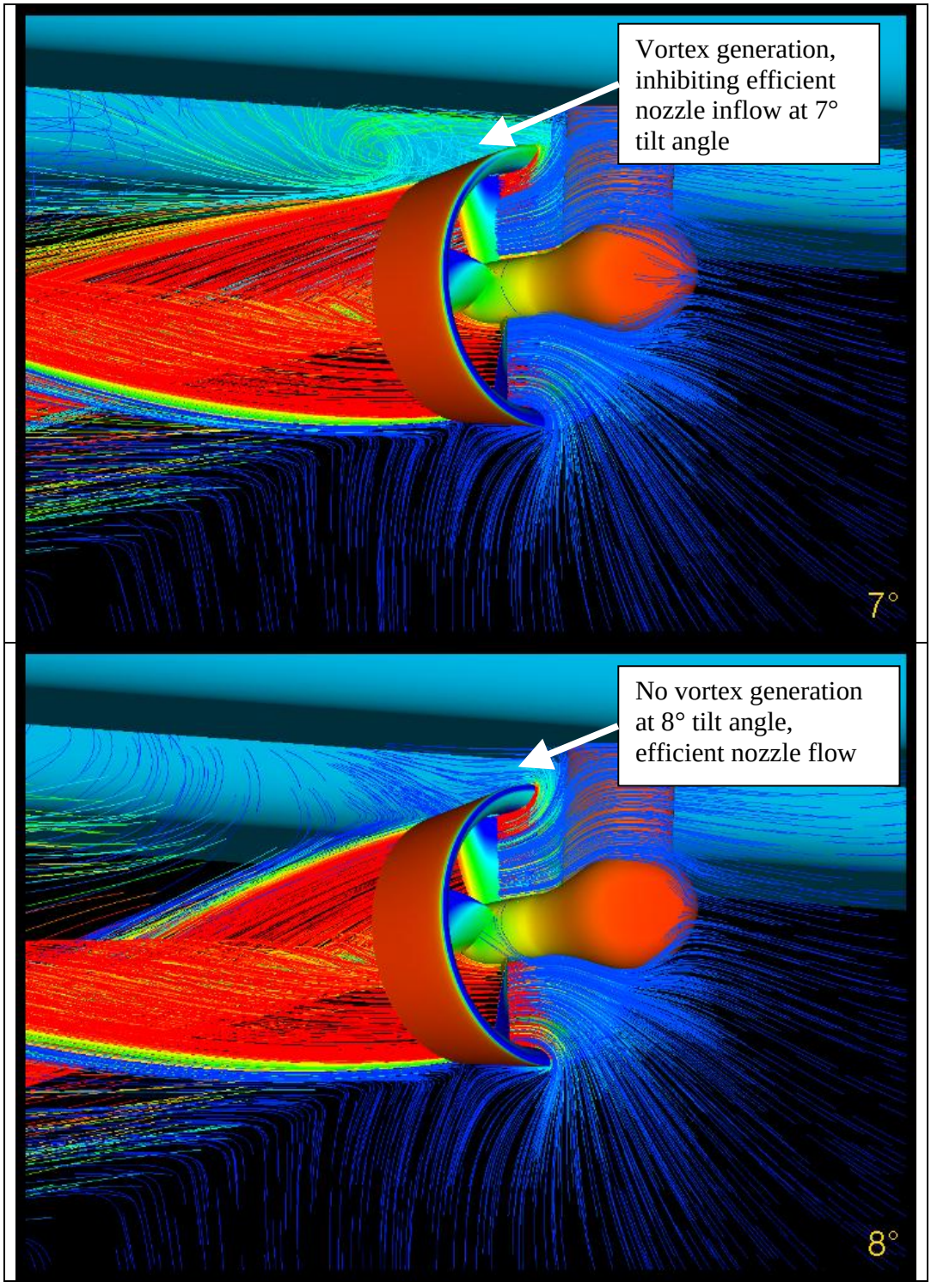

Fig. 7. Flow pattern at 7° and 8° of tilt angle of the propeller shaft

The difference of the flow consists mainly in the vortex between nozzle and pontoon at 7°, which does not exist any more at 8°.

The pressure field at the different tilt angles is shown in figure 8. Red indicates high pressure and blue low pressure. Fig. 8. shows the pressure side of pontoon 2, where the thruster wake creates a stagnation pressure.

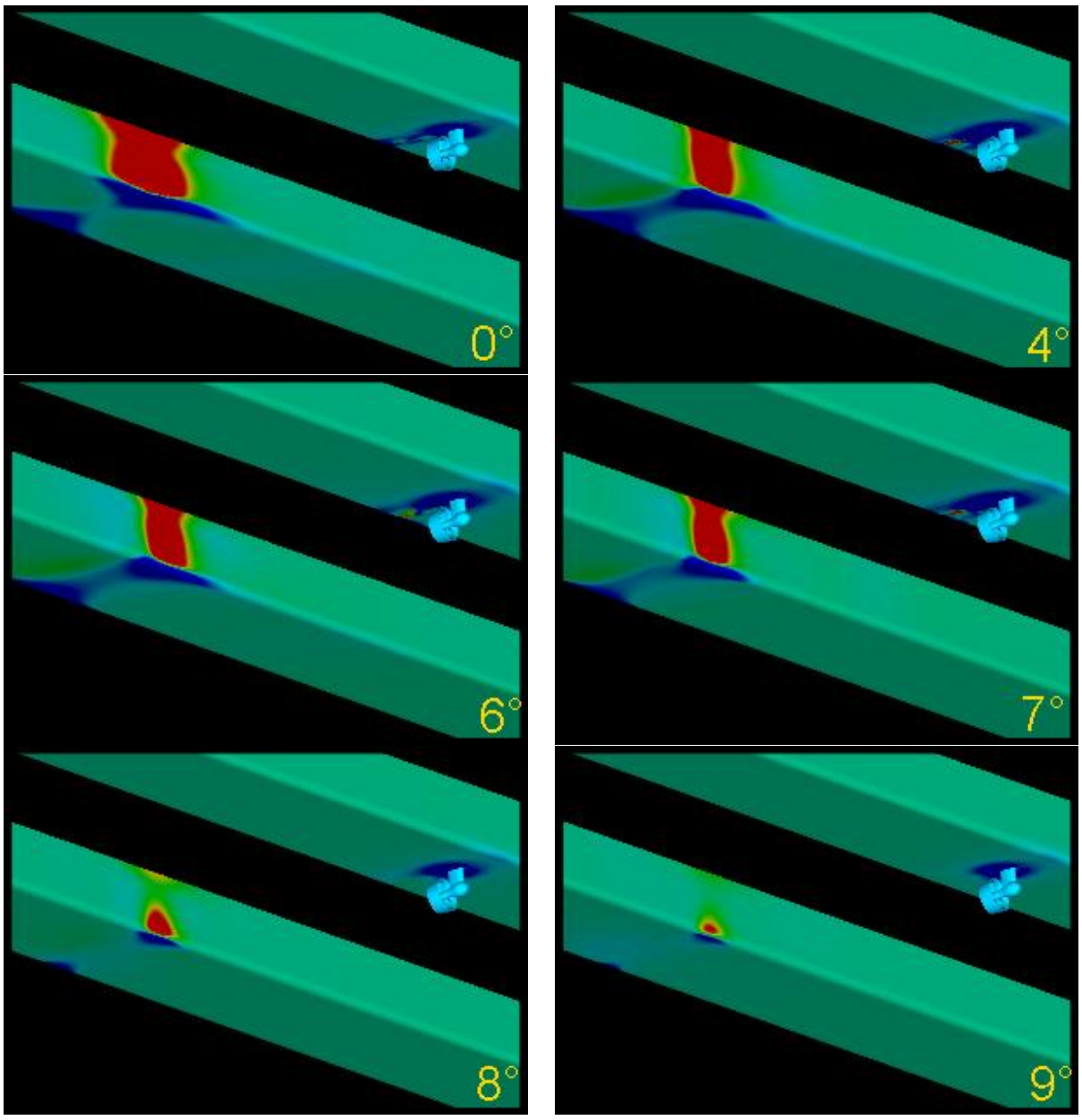

Fig. 8. Pressure distribution (showing the pressure side of pontoon 2)

The areas with high pressure on the second pontoon are reducing as a function of the tilt angle of the propeller axis but it is strongly reduced from 7° to 8°.

Figure 9 shows a view from a different angle and offers insight into the pressure due to the Coanda effect on the pontoon 1. At 8° tilt angle of the propeller shaft the suction force, which reduces the total thrust, is negligible. This gives the conclusion that the Coanda effect on pontoon 1 directs the propeller wake to pontoon 2 and is one source for the high thrust losses.

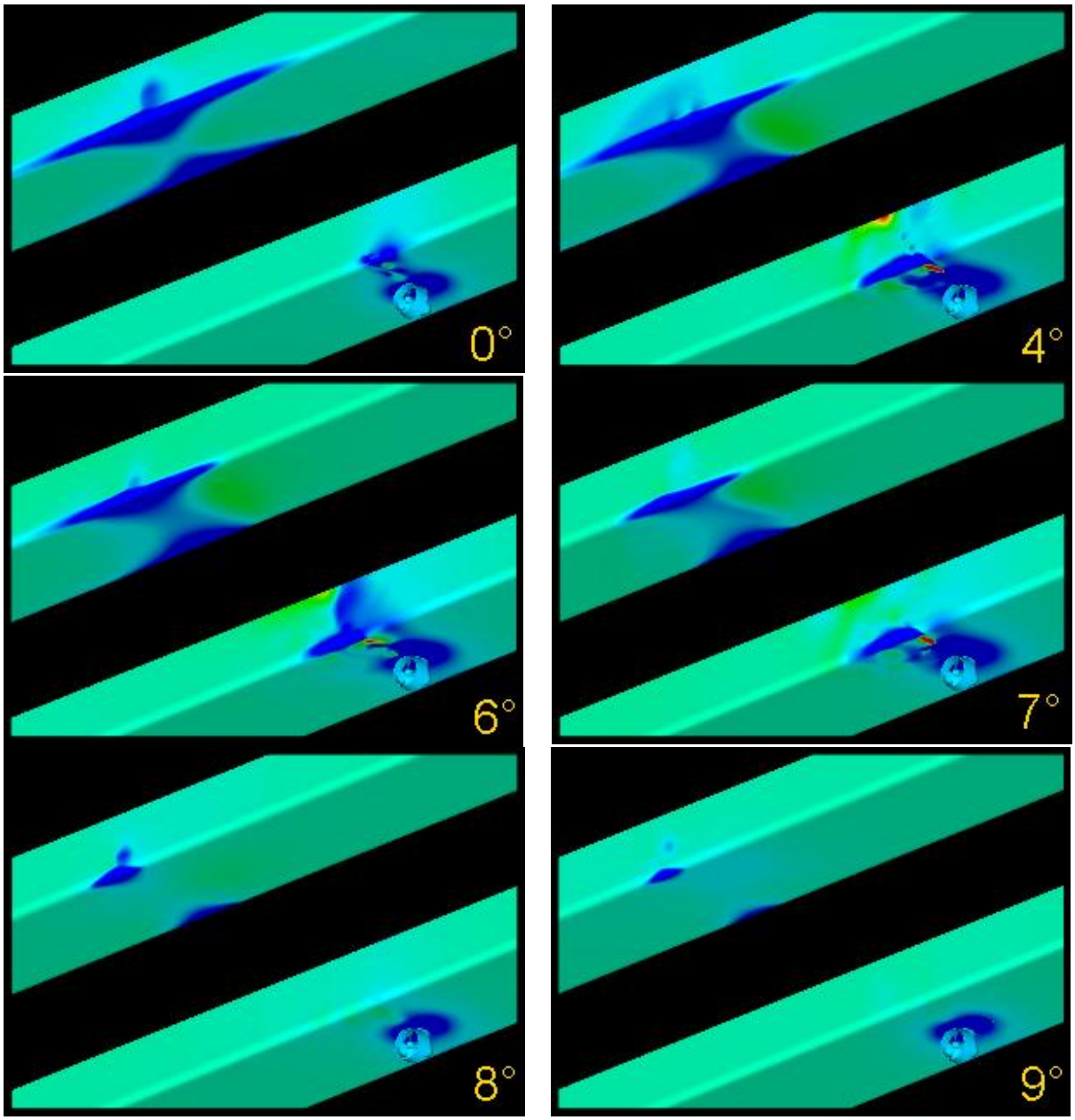

Fig. 9. Pressure distribution (showing the suction side of pontoon 1 and 2)

Does the tilt angle of the propeller shaft also influencing the pressure of the thruster itself? Obviously there is an increase of the thrust because of the increasing tilt angle, as shown in figure 10. The under pressure field of the nozzle is only at 8° tilt angle fully developed.

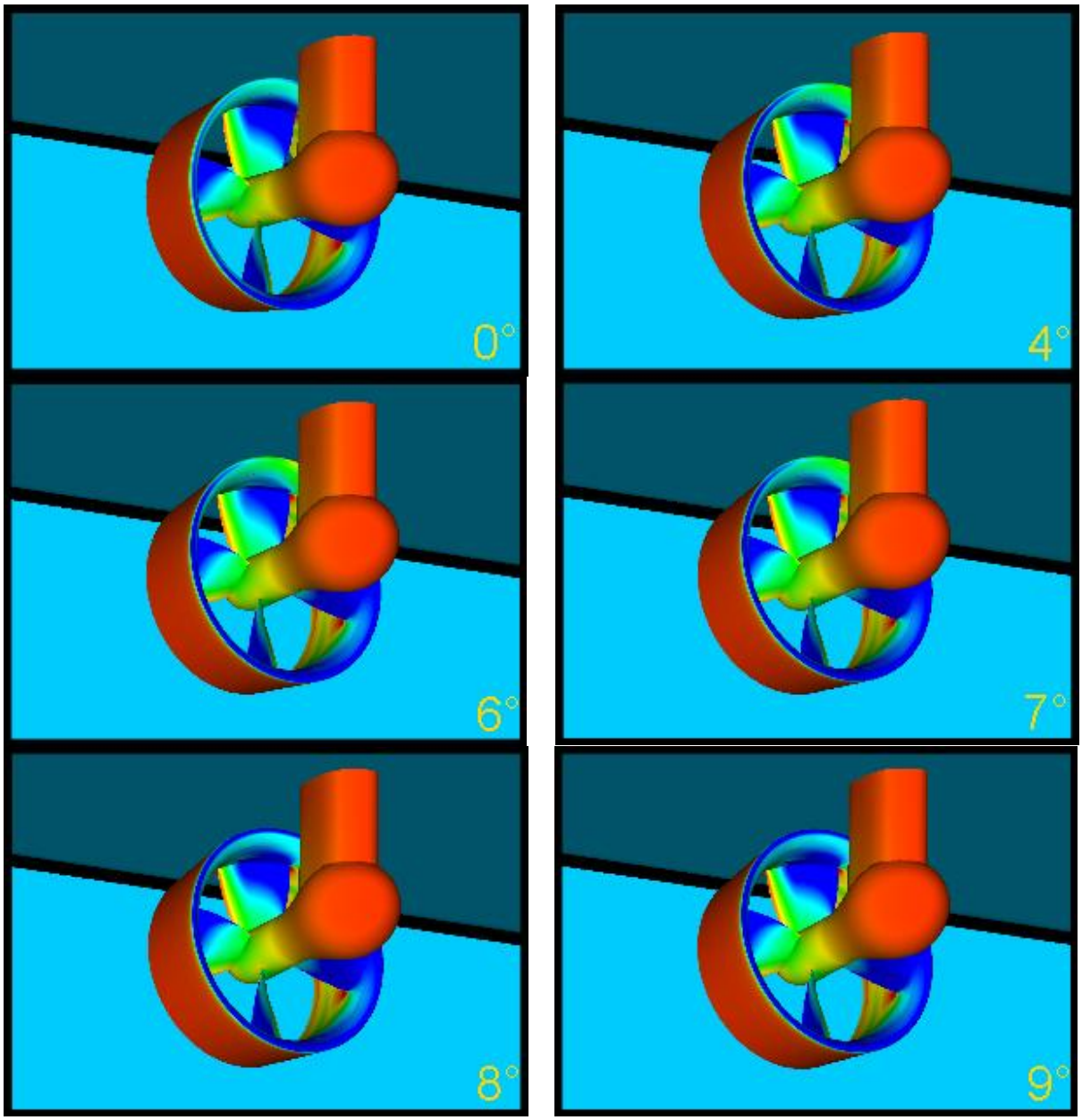

Fig. 10. Pressure Distribution of the azimuthing thruster at different tilt angles of the propeller shaft

The relative forces acting on the pontoon 1 (where the thruster is mounted) and pontoon 2 are shown in figure 11. The maximum force of pontoon 2 at 0° tilt angle is as a reference force scaled, as 100%.

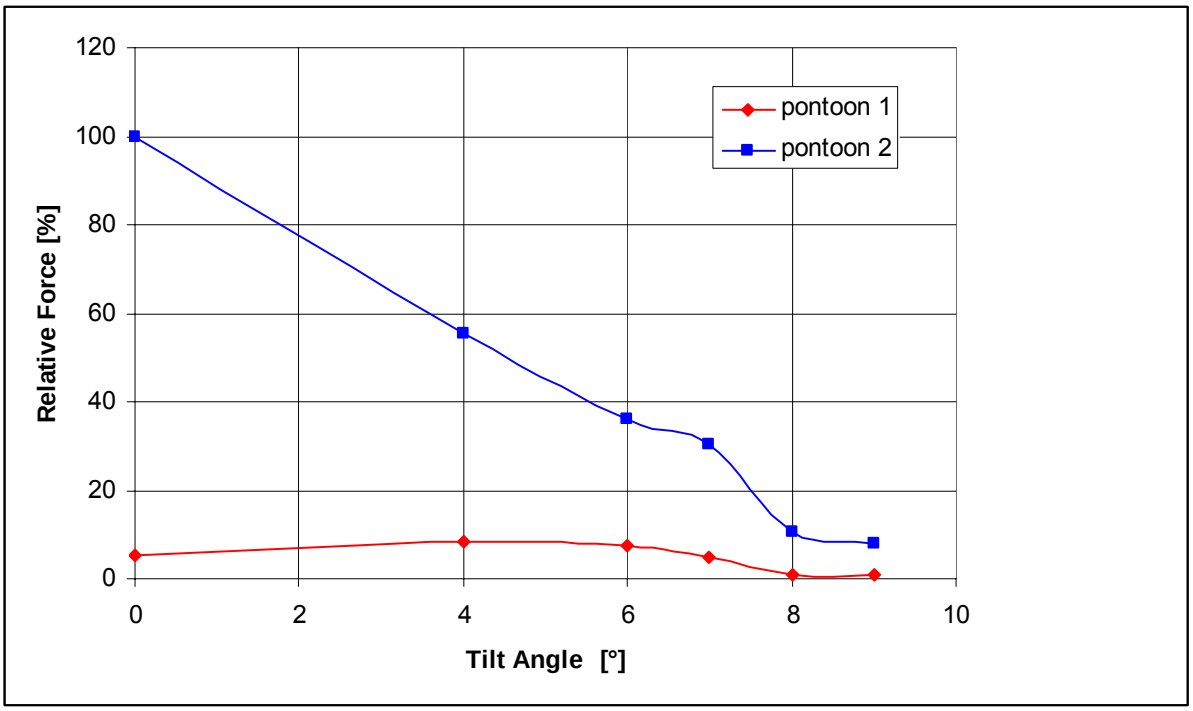

Fig. 11. Transverse forces, acting on both pontoons, the maximum force on pontoon 2 is scaled as 100%.

There is a much higher influence of the tilt angle on pontoon 2 then on pontoon 1. The reason is the high stagnation pressure on the pressure side as shown in figure 8. At 8° the efficiency losses on pontoon 1 is almost zero and on pontoon 2 also very low.

4. Experimental study of the interaction of thruster and hull

Experimental analyses of the thruster hull interaction have been started. These tests are in an early phase; and only the method and first results will be shown here. Voith has a circulating test tank as shown in figure 12.

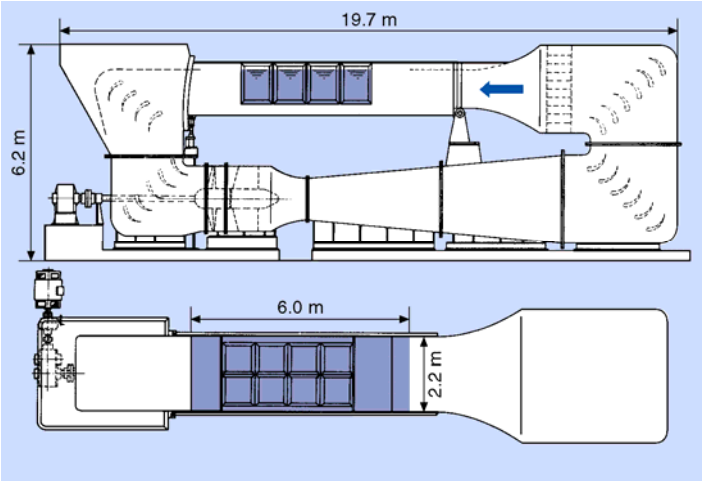

Fig. 12. Tank test facility of Voith Turbo Marine

A steerable thruster, with nozzle, was used for the test. The diameter of the model propeller is 210 mm. The steerable thrust of Voith Schneider Propeller (VSP) is measured by model propellers with a cam cinematic. The VSP models are turned to get the steering forces in all directions. In the same turning facility, the azimuthing thruster has been installed as shown in figure. 13. The measuring system offers a very fast tilting of the propeller axis. Because the measuring system is vertically arranged, the platform was turned 90° for the experiments. The turning of the platform has only little effect on the Coanda effect, which was the focus of the present paper. The free surface effect is not considered correctly and is assumed to be of less influence for the Coanda effect.

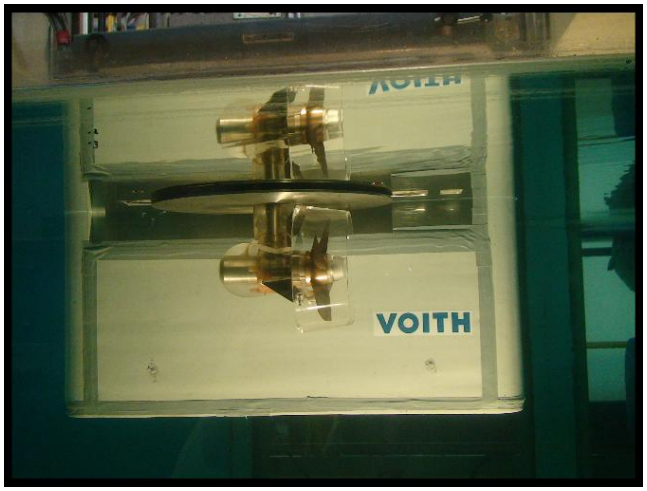

Fig. 13. Measuring arrangement of the 360° steerable thruster

The arrangement of the two pontoons and the thruster is shown in figure 14. The tilt angle has been varied from -6° to + 24°. The distance between the two pontoons was varied for three distances between the pontoons: 1642 mm, 2000 mm and 2358 mm. It was possible to measure at pontoon1 the x- and y-force and in pontoon 2 only the x force.

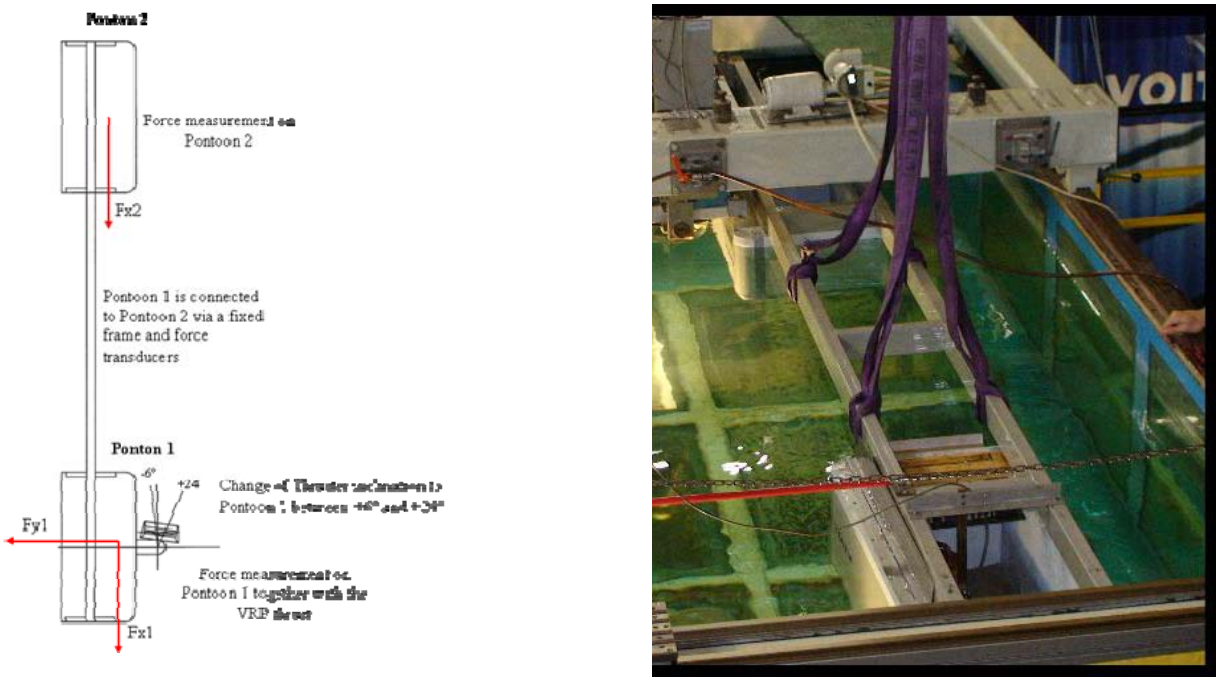

Fig. 14. Test arrangement and definition of the measured forces

The comparison between measured and calculated forces on pontoon 2 is shown in figure 15. There is a good agreement between measurement and calculation for 8° and 9°. At 4° and 6° the measured data and the calculation have a deviation. The reason could be the different Reynolds number or the free surface effect.

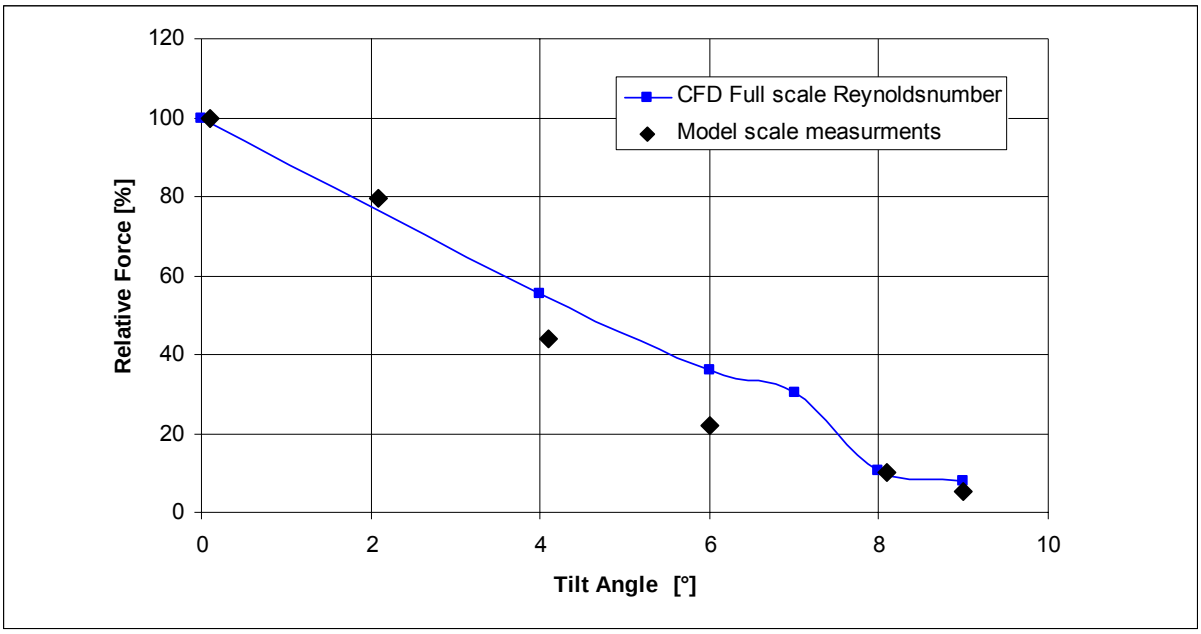

Fig. 15. Transverse forces, acting on pontoon 2; the maximum force on pontoon 2 is scaled as 100%; comparison of full scale CFD calculation and model test data

The flow pattern was in detail analyzed by using ink as shown in figure 16. This allows a detailed study and understanding of the Coanda effect and the separation mechanism at different tilt angels.

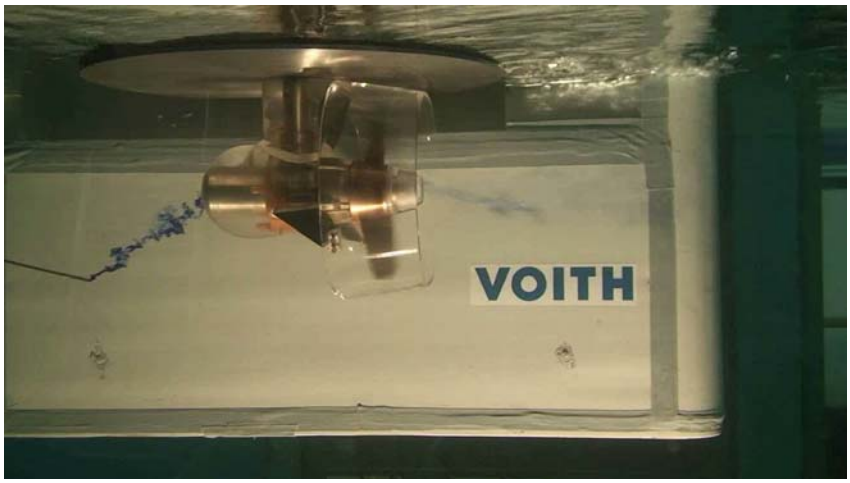

Fig. 16. Visualization of the flow pattern with ink

5. Conclusions

There is a strong influence of the tilt angle of the propeller axis on the thrust losses for azimuthing thrusters. The commercial CFD code has been adapted to calculate the flow field of a thruster and its interaction with two pontoons in transversal direction.

The interesting result of the analyses, valid for the given geometry, was a strong reduction of the thrust losses for a tilt angle of 8°. At 0° the losses can be up to 45% where as at 8° only 5% is lost. This result is in accordance with earlier studies. The present paper gives more insight about the physics of this effect.

A simple experimental method has been developed which allows a fast test of the interaction between a thruster and two pontoons. This method can be used to measure different tilt angles, distances between the pontoons and pontoon shapes. A first comparison shows a reasonable agreement between measurements and calculation.

Future studies are planned. A comparison between model scale and CFD calculation in model scale, including the free surface effect, will be made. Also an optimization of the pontoon shape will be carried out.

The developed methodology offers a fast optimization of offshore platforms and thruster arrangement. It is possible to adapt the CFD technology and the experimental method to other platform and thruster designs. The numerical method will be integrated into a numerical optimization loop.

6. Literature

[1] Jürgens, D.; Palm, M.; Perić, M. ; Schreck, E.
Prediction of Resistance of Floating Vessels
MARINE CFD 2008; SOUTHAMPTON, 26.-27. MARCH 2008

[2] Jürgens, D.; Caspersen, B.
Future Voith Water Tractor Development using sophisticated simulation models
Tugnology, Southampton, 11.-12. June 2007

[3] Vartdal, L.; Garen, R.
A Thruster System which Improves Positioning Power by Reducing Interaction Losses
Dynamic Positioning Conference, Sept. 2001

[4] Moltrecht, T.; Albers, T.
Ruderpropeller für Offshoreanwendungen
Schiff & Hafen, Nr. 8, August 2007

[5] Lehn, E.
Thruster Interaction Effects
Ship Research Institute of Norway Report R-102.80, 1980

[6] Lehn, E.
Thruster-Hull Interaction Effects
Ship Research Institute of Norway Report R-119.81, 1981

[7] Lehn, E.
On the Propeller Race Interaction Effects
Ship Research Institute of Norway Report P-01.85, 1985

[8] Lehn, E.
Practical Methods for Estimation of Thrust Losses
Project Report FPS 2000, Mooring and Positioning, Summary Report Part 1.6,
MARINTEK, 1992

[9] Mattila, M.; Ylitalo, J.; Soles, J.
The Reliable Solution with Minimal Thrust Losses
Dynamic Positioning Conference, Sept. 2002

[10] Vartdal, L.; Garen, R.
A Thruster System which Improves Positioning Power by Reducing Interaction Losses
Dynamic Positioning Conference, Sept. 2001

[11] Abdel-Maksoud, M.; Heinke, H.-J.
Scale Effects on Ducted Propellers
24th Symposium on Naval Hydrodynamics, Fukuoka, Japan, July 2002

[12] Jürgens, D.; Grabert, R.
New Hydrodynamic Aspects of Double-ended Ferries with Voith Schneider Propeller
2nd International conference on Double Ended Ferries, Norway, Alesund, March 2003